

3D QSAR AND MOLECULAR DOCKING STUDIES OF STRUCTURALLY DIVERSE ESTROGEN RECEPTOR LIGANDS

MD ATAUL ISLAM, ARUP MUKHERJEE, ACHINTYA SAHA*

Department of Chemical Technology, University of Calcutta, 92, A.P.C.Road, Kolkata 700009, India. Email: achintya_saha@yahoo.com

Received: 28 Oct 2011, Revised and Accepted: 22 Dec 2011

ABSTRACT

Hormone-responsive breast cancer is one of leading cause of cancer death world wide in the women community. The female sex hormone estrogen primarily controls the development of female sex characteristics including division of breast cell. This hormone exerts its effects after binding to estrogen receptor (ER), which is nuclear-activated transcription factor. The present study is considered to explore important pharmacophore signals for binding affinity of estrogen ligands using molecular field (CoMFA) and similarly analyses (CoMSIA), substantiated with molecular docking study. Both CoMFA ($R^2=0.974$, $se=0.240$, $Q^2=0.589$, $R^2_{pred}=0.612$) and CoMSIA ($R^2=0.997$, $se=0.088$, $Q^2=0.703$, $R^2_{pred}=0.624$) models suggest that steric and electrostatic factors are crucial for binding affinity. Further, the similarity analysis and docking studies revealed that hydroxyl and alkyl groups are important for formation of potential interactions at the active site cavity of the ER.

Keywords: Estrogen, CoMFA, CoMSIA, Molecular docking.

INTRODUCTION

The estrogen belongs to the sex steroid hormones, secreted by the ovaries and testis with involvement of placenta, adipose tissue, and adrenal glands¹. Among the several structurally related forms 17 β -estradiol is found as predominant. Estrogen plays crucial role in female reproductive system and also exerts important effects on nonreproductive targets such as bone, cardiovascular system and neural sites involved in cognition². It is also reported that estrogen influence the brain centers that maintain body temperature, and enable the vaginal lining to stay thick and lubricated³. Due to loss of estrogen production after menopause, hot-flushes, vaginal atrophy and sleeping disturbance arise, and also rise of low-density lipoprotein (LDL) that progressively increases the chance of coronary and osteoporosis diseases⁴. The hormone replacement therapy (HRT) in which synthetic estrogens are administered into the body that reduce osteoporotic fractures and improve severe menopausal symptoms⁴, but on other hand malevolent aspect of HRT is increasing chance of breast and uterin cancers^{5,6}. Presently there are three strategy for treatment of hormone-responsive breast cancer, such as inhibition estrogen from binding to its main target estrogen receptor (ER) using antiestrogen, e.g. tamoxifen⁷; preventing its synthesis using aromatase inhibitor⁸; and down-regulating ER protein level using pure antiestrogen, e.g. fulvesteron⁹.

Estrogen mediates its biochemical mechanism in target tissues after binding to intracellular receptor proteins ER^{10,11}, which is a nuclear ligand-activated transcription factor¹². ER constituted similar architecture to the other 50-60 members of the steroid/thyroid hormone receptor family¹²⁻¹⁴ and comprises six distinct domains A-F. The ligand binding domain (LBD) consisting E/F domain at the carboxy terminal and responsible for ligand binding, receptor dimirization, nuclear translocation and transactivation of target gene expression via activation function - 2 (AF-2)^{13,14}. The AF-2 region comprises of 12 α -helices, which form a hydrophobic pocket responsible for binding of ligand¹⁵ and fundamental in distinguishing between agonist and antagonist functions¹⁶ of ER. Knowledge of ER has permitted the modeling of estrogenic activity using different chemometric techniques. The structural requirement for binding of steroid to ER is essential both for design of new drug and to evaluate the health risk of chemical of ER affinity¹⁷. The chemometric drug design (CDD) is widely

used to design lead molecules involving two important techniques, ligand-based and structure-based approaches. When the properties of the ligands are analyzed without any information of receptor site is known as ligand-based drug design (LBDD), while the ligands are designed with help of receptor site is called structure-based drug design (SBDD). Researchers are devoted to search potent molecules for treatment of post-menopausal diseases using both LBDD and SBDD approaches. Our group has explored the prime pharmacophore signals for estrogen mediated bioactivities of different groups of structural congeneric compounds through Quantitative Structure Activity Relationships (QSAR) studies¹⁸⁻²¹. Molecular docking and QSAR studies of estrogen ligands are also explored for potent antiestrogens in several studies^{22,23}. On the availability of the crystal structure of active site both ligand-based and structure-based studies will be powerful methods to design lead compound. The present work is considered to explore both approaches for a set of structurally diverse compounds^{24,25} with respect to binding affinity to ER.

MATERIALS AND METHODS

The main objective of the work is to find out correlation between chemical structure with biological activity of the molecules using Partial Least Square (PLS) method and potential interactions between ligand and active site of the receptor molecule. The binding affinity for QSAR study is expressed as $kRBA = \log_{10}(100 \times RBA)$. The dataset (Table 1) is randomly divided into training set ($n_{tr}=25$) containing most and least active compounds, and test set ($n_{ts}=10$) to validate the derived models in QSAR study. The different control parameters are used to check the superiority of 3D QSAR models are: R^2 (correlation coefficient), se (standard error of estimate), Cross-validated variance (CVV) Q^2 (Leave-One-Out (LOO) cross-validated²⁶ correlation), F (variance ratio) with df (degree of freedom), R^2_{bs} (bootstrapped correlation coefficient) and s_b (standard error of bootstrapped correlation). To evaluate the predictive power of the model, R^2_{pred} and s_p (standard error of prediction) of the test set are also estimated. In case of docking study GlideScore²⁷ and interactions between ligand and receptor are considered for best pose selection.

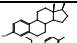
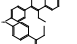
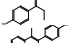
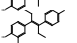
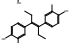
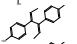
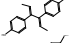
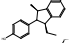
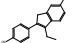
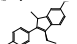
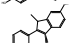
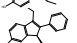
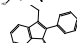
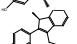
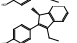
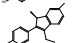
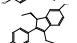
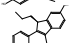
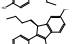
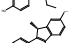
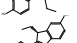


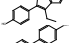
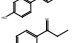
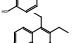
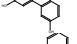
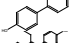
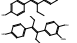
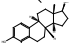
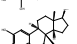
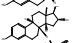
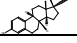

3D QSAR

QSAR is mathematical robust model which attempts to find a statistically significant correlation between chemical structure and biological activity²⁸. 3D QSAR is a ligand-based approach which

includes Comparative Molecular Field Analysis (CoMFA)²⁹ and Comparative Molecular Similarity Indices Analysis (CoMSIA)³⁰, and both analysis techniques reported as effective for understanding of structure-activity relationship, useful to predict the biological activity before synthesis and animal experiment³¹, lead optimization and drug-target interaction. In molecular field analysis (CoMFA), steric and electrostatic interaction energies³² are calculated using Lenard-Jones

and Coulombic potentials, and correlated with biological activity of the molecules. In case of CoMSIA study, similarity indices are calculated at regularly placed grid points of the aligned molecules, and additionally hydrogen bond (HB) acceptor and donor along with hydrophobic fields are incorporated³³. The contour maps of both methods are used to get general insights into the topological features of the binding site.

Table 1: Observed and predicted relative binding affinity (RBA) to the receptor of estrogen ligand

Comp. No.	Ligand	Smiles	Obs. ¹	Predicted activity (CoMFA)	Predicted activity (CoMSIA)	Glide Score
1		<chem>CC12CCC3C(Cc4cc(ccc43)O)C2CCC1O</chem>	100.000	95.280	86.696	-8.420
2		<chem>CC\C(c1ccc(cc1)O)=C(\CC)/c1ccc(cc1)O</chem>	288.400	133.968	194.536	-8.810
3		<chem>CC/C(c1ccc(cc1)O)=C(\CC)/c1ccc(cc1)O</chem>	0.790	0.418*	0.427*	-5.600
4		<chem>C/C(=C(/C)\c1ccc(cc1)O)/c1ccc(cc1)O</chem>	33.110	19.770	34.834*	-6.670
5		<chem>CC\C(c1ccc(cc1)O)=C(\CC)/c1ccc(c(c1)O)O</chem>	100.000	99.083	104.472	-11.170
6		<chem>CC\C(c1ccc(c(c1)O)O)=C(\CC)/c1ccc(c(c1)O)O</chem>	25.120	133.968	19.454*	-10.250
7		<chem>C/C=C(/c1ccc(cc1)O)\C(=C(/C)\c1ccc(cc1)O)</chem>	0.300	0.308	0.299	-6.240
8		<chem>C\C=C(/c1ccc(cc1)O)\C(=C(\C)\c1ccc(cc1)O)</chem>	19.950	12.647*	8.913*	-6.230
9		<chem>CCC1C(C(C)c2cc(ccc12)O)c1ccc(cc1)O</chem>	2.000	1.069	2.158	-9.730
10		<chem>CCC1=C(Cc2cc(ccc12)O)c1ccc(cc1)O</chem>	13.800	15.311	10.520	-9.330
11		<chem>CCC1=C(C(C)c2cc(ccc12)O)c1ccc(cc1)O</chem>	100.000	28.119*	162.555*	-8.780
12		<chem>CCC1=C(C(C)c2cc(ccc12)O)c1ccc(cc1)O</chem>	141.250	83.176*	83.176*	-9.660
13		<chem>CCC1=C([C@@H](C)c2cc(ccc12)O)c1cccc1</chem>	1.820	1.954*	1.429*	-9.040
14		<chem>CCC1=C([C@H](C)c2cc(ccc12)O)c1cccc1</chem>	0.200	0.084*	0.331	-9.070
15		<chem>CCC1=C([C@@H](C)c2cccc12)c1ccc(cc1)O</chem>	5.620	4.721*	6.950	-8.120
16		<chem>CCC1=C([C@H](C)c2cccc12)c1ccc(cc1)O</chem>	0.890	0.226	1.028*	-8.500
17		<chem>CCC1=C([C@@H](C)c2cc(ccc12)O)c1ccc(cc1)O</chem>	288.400	326.588	304.790	-8.7100
18		<chem>CC[C@H]1c2cc(ccc2C(=C1c1ccc(cc1)O)CC)O</chem>	295.102	230.144	301.995	-10.110
19		<chem>CCC[C@H]1c2cc(ccc2C(=C1c1ccc(cc1)O)CC)O</chem>	22.090	208.449	182.390	-12.180
20		<chem>CCCC[C@H]1c2cc(ccc2C(=C1c1ccc(cc1)O)CC)O</chem>	177.803	131.220	231.740	-12.410
21		<chem>CCC1=C([C@H](C)c2cc(ccc12)O)c1ccc(cc1)O</chem>	12.880	28.119	16.255	-9.530
22		<chem>CC[C@@H]1c2cc(ccc2C(=C1c1ccc(cc1)O)CC)O</chem>	10.960	20.464*	16.218	-9.850
23		<chem>CCC[C@@H]1c2cc(ccc2C(=C1c1ccc(cc1)O)CC)O</chem>	18.200	63.241	17.906	-10.990
24		<chem>CCCC[C@@H]1c2cc(ccc2C(=C1c1ccc(cc1)O)CC)O</chem>	7.940	6.442	7.691	-12.120
25		<chem>Oc1ccc(cc1)c1ccc(cc1)O</chem>	0.020	0.069	0.017	-7.580
26		<chem>CCC(=O)c1ccc(cc1)O</chem>	0.100	0.062	0.101	-5.600
27		<chem>CCc1c(c2ccc(cc2c2cc(ccc12)O)O)CC</chem>	0.160	0.147	0.169	-7.010
28		<chem>Oc1ccc(cc1)c1cccc1</chem>	0.020	0.017	0.019	-12.410
29		<chem>CC\C(=C(\CC)/c1ccc(cc1)O)\c1ccc(cc1)OC</chem>	19.950	15.241	22.491	-8.240
30		<chem>CC/C(=C(/CC)\c1ccc(c(c1)OC)O)/c1ccc(cc1)O</chem>	10.000	21.727*	8.670	-9.650
31		<chem>CC12CCC3C(Cc4c(c(ccc43)O)O)C2CC[C@@H]1O</chem>	52.900	42.170	60.117*	-10.480
32		<chem>CC12CCC3C(Cc4cc(c(cc43)O)O)C2CC[C@@H]1O</chem>	22.400	63.826*	22.751	-11.290
33		<chem>CC12CCC3C(Cc4cc(ccc43)O)C2C[C@@H](O)[C@@H]1O</chem>	9.720	13.062	9.931	-8.690
34		<chem>CC12CCC3C(Cc4cc(ccc43)O)C2CCC1(O)C#C</chem>	190.000	133.045	179.473	-10.250

35



CC12CCC3C(CCc4cc(ccc43)O)C2CCC1=O

7.310

8.630

6.918

-8.900

¹Observed activity^{24,25}; *test compounds

To develop robust CoMFA/CoMSIA models, conformer selection and molecular alignment are important factors. The molecules of data set are expected to be aligned against each other to maximize the overlap of the pharmacophores to generate molecular fields correctly³⁴. If the crystal structure of target proteins is available then molecular docking is the solution of alignment of molecules for development of 3D QSAR models. It is reported that docking conformers are appropriately aligning the ligands and developing reliable QSAR models^{35,36}. As crystal structure of ER are available in RCSB Protein Data Bank³⁷, combination of molecular docking and 3D QSAR approach would be desired for development of potent ER ligands. Individual molecules of dataset are docked with crystal structure of ER (PDB ID: 3OMO³⁸) respectively obtained from Protein Data Bank³⁷, and best docked conformer of each compound has been considered for 3D QSAR studies. In case of CoMFA, fields are generated using steric ('s') and electrostatic ('e') interactions, and calculated on a regular space grid of 3Å. Values of the field are truncated at 30.0 kcal/mol. Partial atomic charges are calculated by the Gasteiger-Huckel method³⁹. In case of CoMSIA, 's', 'e' and hydrophobic ('p') parameters are considered together with hydrogen bond (HB) acceptor ('a') and donor ('d') factors.

Molecular Docking

In molecular docking method, ligand interacts to the protein or nucleic acid target and provides a conceptual frame work for designing the desired potency and specificity of potential drug leads for a given therapeutic target. Main objective of docking procedures is to identify correct poses of ligands in the binding pocket of a protein and to predict the affinity between the ligand and protein. A number of algorithms^{40,41} can be used for docking which include matching ligand and receptor complementary surfaces or the calculation of the ligand-receptor interaction energies. The method validates ligand-receptor interacting ability by the calculation of scoring functions. Docking can be performed by placing rigid molecules or fragments into the protein's active site using different approaches like clique-search⁴², geometric hashing⁴³ or pose clustering⁴⁴.

Molecular docking of the data set is performed to understand detailed binding modes of ligands to ER. In the present study, the Grid-Based Ligand Docking with Energetics (Glide) algorithm that approximates a systematic search of positions, orientations, and conformations of the ligand in the receptor binding site using a series of hierarchical filters^{27,45,46} are used. The grid represents the

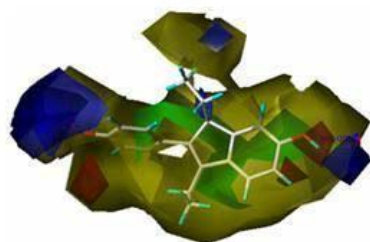
shape and properties of the receptor by several different sets of fields, computed prior to docking and provides progressively more accurate scoring of the ligand pose. The binding site is defined by a rectangular box which keeps the mass centre of the ligand within the box. Conformers are generated through an exhaustive search of the torsional minima, and the conformers followed by clustered in a combinatorial fashion. After that each cluster, characterized by a common conformation of the "core" and an exhaustive set of "rotamer group" conformations, is docked as a single object in the first stage²⁷. Narrows the search space and reduces the number of poses due to searching with a rough positioning and scoring phase and retain only hundreds. Further the selected poses are minimized on pre-computed OPLS-AA van der Waals and electrostatic grids for the receptor⁴⁷. Finally about 5-10 lowest-energy poses obtained are subjected to a Monte Carlo procedure in which nearby torsional minima are examined, and the orientation of peripheral groups of the ligand is refined⁴⁷. The score of the minimized poses is rescored using the GlideScore function along with force field-based components and additional terms accounting for solvation and repulsive interactions. The best pose considered using a model energy score (Emodel) that combines the energy grid score, GlideScore, and the internal strain of the ligand²⁷.

RESULTS AND DISCUSSION

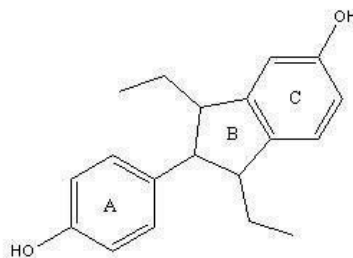
3D QSAR

CoMFA

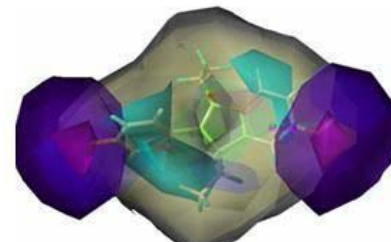
The best model ($R^2=0.974$, $se=0.240$, $Q^2=0.589$, $R^2_{pred}=0.612$) for field analysis is obtained with contribution of 's' (42.60%) and 'e' (57.40%) factors (Fig. 1A). The statistical results are depicted in Table 2. The regions of green contour suggest that substituents imparting steric influence in these positions might improve the biological activity, while the yellow region indicates that an increased steric influence is unfavorable for the binding affinity. Two phenyl ('A' and 'C' in Fig. 1B) and one acyclic ('B') rings are sterically favorable for the binding interactions at the active site cavity, whereas rest of the surface areas are sterically unfavorable regions. Vicinity to the hydroxyl groups attached to the rings 'A' and 'C' (Fig. 1B), and alkyl group attached to the ring 'B' impart the electronic charges are favorable for electrostatic interactions with the receptor. The observed vs. predicted activity is depicted in Fig. 2. Good predicted correlation value ($R^2_{pred}=0.612$) of the test compounds confirms the suitability of the model selection.



A



B



C

Steric:

Green favorable, yellow unfavorable

Electrostatic: Blue favorable, red unfavorable
 Hydrophobic: Cyan favorable, White unfavorable
 Acceptor: Magenta favorable, purple unfavorable

Fig. 1: Mapped features of CoMFA (A) and CoMSIA (C) studies fitted with most active compound (B) of the dataset

Table 2: Statistical results of 3D QSAR study of estrogen receptor ligands.

Parameters	CoMFA	CoMSIA
n_{tr}	25	25
Components	5	7
R^2	0.974	0.997
se	0.240	0.088
$F(df)$	112.906 (6,18)	705.654 (7,17)
Contributions (%)		
s	0.426	0.133
e	0.574	0.396
p	-	0.249
a	-	0.221
Q^2	0.589	0.703
R^2_{bs}	0.989	0.999
S_{bs}	0.169	0.050
R^2_{pred}	0.612	0.624
S_p	0.321	0.389

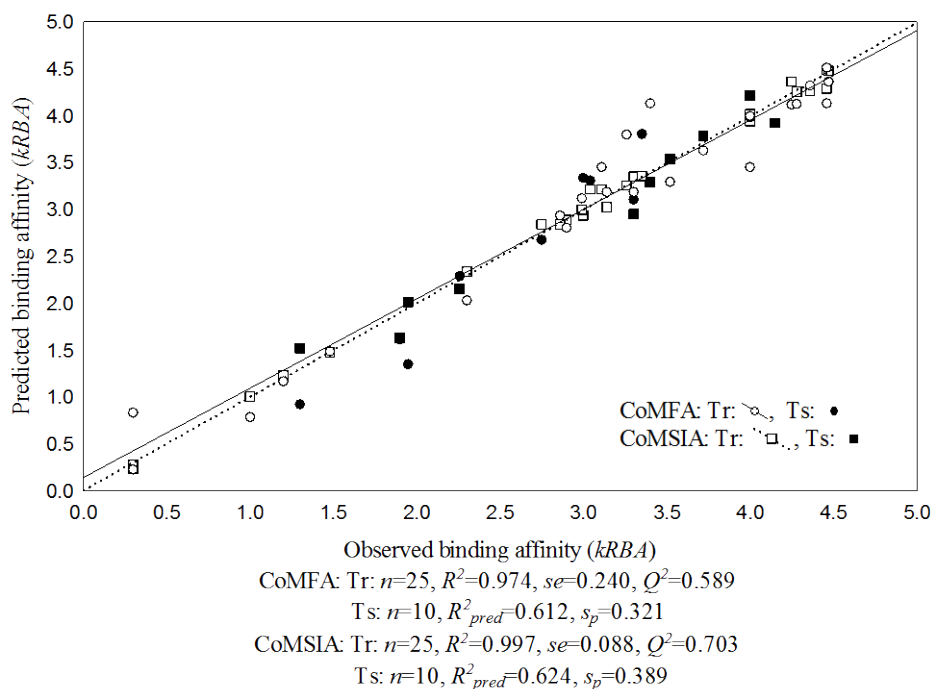


Fig. 2: Observed vs. predicted binding affinity of estrogen receptor ligands as per CoMFA and CoMSIA studies.

CoMSIA

The best model ($R^2=0.997$, $se=0.088$, $Q^2=0.703$, $R^2_{pred}=0.624$) for similarity study is obtained with combined contribution of 's' (13.30%), 'e' (39.60%), 'p' (24.90%) and HB 'a' (22.10%) factors (Fig. 1C). Phenyl rings 'A' and 'C' impart steric and hydrophobic properties of the molecule and favorable for formation of steric and hydrophobic interactions of the receptor site, but rest of the surface areas show unfavorable for both steric and hydrophobic properties. Due to increase of electron density surrounding the phenyl rings ('A' and 'C')

show favorable for electrostatic interactions, but hydroxyl groups attached to same and alkyl group attached to the cyclopentane ring ('B') have negative influence for electrostatic factor. Hydroxyl groups attached to the phenyl rings are behaved as HB acceptors suggesting hydrogen bond interactions with amino acid residues at the active site. The observed vs. predicted activity is delineated in Fig. 2. Good correlation value ($R^2_{pred}=0.624$) of the test compounds proves robustness of the CoMSIA Model.

Molecular Docking

Molecular docking is performed to visualize the potential interactions between ligand and catalytic residues of ER (PDB ID: 3OM0³⁸). The docking result is characterized on the basis of GlideScore (Table 1) and interactions observed at the active site cavity. The docked pose of most active compound (Comp. 18) is depicted in Fig. 3. Theoretically more negatively scoring compounds are better binders, and it is observed that all compounds in the data set docked at the active site with high negative score.

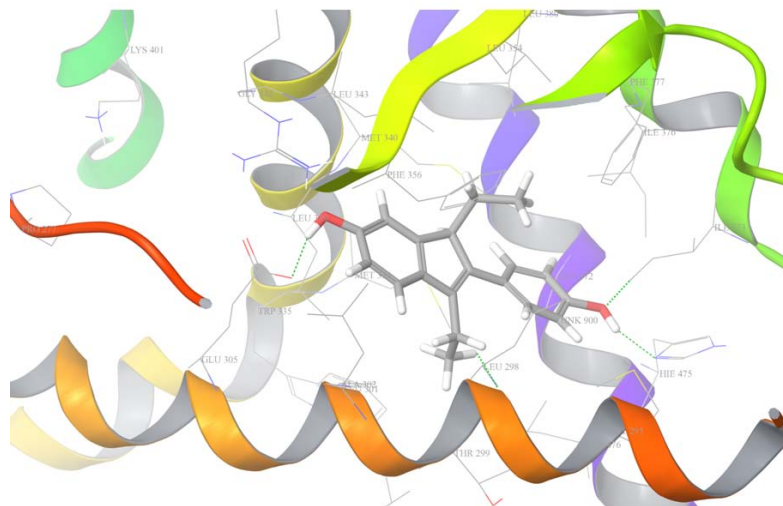


Fig. 3: Molecular docking interactions at the binding site ER with most active compound (Comp. 18)

The docked pose of comp. 18 (Fig. 3) explain that polar Trp335 and His475, and non-polar Leu298 and Ile373 are catalytic residues at the active site revealed as crucial for binding interactions. Presence of electronegative hydroxyl group attached to ring 'A' interacts with His475 and Ile373 by forming potential hydrogen bonding, whereas hydroxyl group attached to ring 'C' is formed HB interaction with Trp335. The bulky alkyl group attached to ring 'B' generates the hydrophobic core also found crucial for interaction with non-polar residue Leu298.

The docking study also correlates the functionality developed in 3D QSAR and space modeling⁴⁸ studies. The rings 'A' and 'C' found as sterically and electrostatically favorable in CoMFA study, additionally ring 'B' revealed as important for steric interaction. Similarly rings 'A' and 'C' are important for steric, hydrophobic and electrostatic interactions in CoMSIA study. Moreover hydroxyl groups attached to the phenyl rings 'A' and 'C' act as HB acceptors for interaction with active site cavity for both CoMSIA and space modeling⁴⁸ studies. Bulky alkyl group attached to ring 'B' imports hydrophobicity also depicted in pharmacophore study⁴⁸. Observations in both 3D QSAR and space modeling studies are substantiated by the HB interactions between hydroxyl group attached to rings 'A' and 'C' with Trp335 and, Ile373 and His475 respectively, whereas hydrophobic interaction portrayed between alkyl group attached at ring 'B' and Leu298.

CONCLUSION

In the present work, CoMFA and CoMSIA approaches of 3D QSAR and molecular docking studies are adopted to rationalize the ER binding affinity and molecular interactions of structurally diverse estrogen receptor ligands. The 3D QSAR studies revealed that steric and electrostatic features are prime factors for binding affinity. Both field and similarity analyses models show good predictive ability to test compounds. The contour maps show good compatibility with the

From Table 1, it is illustrated that comps. 20 and 28 have highest negative score -12.410 followed by comp. 24 (-12.120) and comp. 19 (-12.180). Comps. 3 and 25 each give lowest negative score -5.600 followed by comp. 8 (-6.230) and comp. 7 (-6.240). The most active compound (comp. 18) gives GlideScore of -10.110 and least active compounds (comps. 25 and 28) generate -7.580 and -12.410 respectively.

receptor properties and explain the crucial regions for steric, electrostatic, hydrophobic and HB interaction with the receptor site. The significant GlideScore supports that molecules of the data set are successfully interacted with right conformation. The docked poses illustrate that hydroxyl and alkyl groups present in the molecular system are important for binding interaction.

ACKNOWLEDGEMENT

One of the author, Md A. Islam wishes to thank CSIR, New Delhi, India for awarding Senior Research Fellowship.

REFERENCES

- Lewis JS, Jordan VC. Selective estrogen receptor modulators (SERMs): mechanisms of anticarcinogenesis and drug resistance. *Mutat Res* 2005; 591: 247-63.
- Lindzey J. Expression and Function of Estrogen Receptors-alpha and beta. In: Manni A, Verderame M, editors. *Selective Estrogen Receptor Modulators*. New Jersey: Humana Press; 2002. p. 29-56.
- Maggi A, Ciana P, Belcredito S, Vegeto E. Estrogens in the nervous system: mechanisms and nonreproductive functions. *Annu Rev Physiol* 2004; 66: 291-313.
- Rossouw JE, Anderson GL, Prentice RL, LaCroix AZ, Kooperberg C, Stefanick ML, et al. Risks and benefits of estrogen plus progestin in healthy postmenopausal women: principal results From the Women's Health Initiative randomized controlled trial. *JAMA* 2002; 288: 321-33.
- Gehrig PA, Bae-Jump VL, Boggess JF, Groben PA, Fowler WC, Jr., Van Le L. Association between uterine serous carcinoma and breast cancer. *Gynecol Oncol* 2004; 94 :208-11.
- Chlebowski RT, Hendrix SL, Langer RD, Stefanick ML, Gass M, Lane D, et al. Influence of estrogen plus progestin on breast cancer and mammography in healthy postmenopausal women: the Women's Health Initiative Randomized Trial. *JAMA* 2003; 289: 3243-53.

7. Tamoxifen for early breast cancer: an overview of the randomised trials. Early Breast Cancer Trialists' Collaborative Group. *Lancet* 1998; 351: 1451-67.
8. Coombes RC, Gibson L, Hall E, Emson M, Bliss J. Aromatase inhibitors as adjuvant therapies in patients with breast cancer. *J Steroid Biochem Mol Biol* 2003; 86: 309-11.
9. Johnston S. Fulvestrant and the sequential endocrine cascade for advanced breast cancer. *Br J Cancer* 2004;90 Suppl 1: S15-8.
10. Enmark E, Gustafsson JA. Oestrogen receptors - an overview. *J Intern Med* 1999; 246: 133-8.
11. Pearce ST, Jordan VC. The biological role of estrogen receptors alpha and beta in cancer. *Crit Rev Oncol Hematol* 2004; 50: 3-22.
12. Evans RM. The steroid and thyroid hormone receptor superfamily. *Science* 1988; 240: 889-95.
13. Giguere V. Orphan nuclear receptors: from gene to function. *Endocr Rev* 1999; 20: 689-725.
14. Beato M, Klug J. Steroid hormone receptors: an update. *Hum Reprod Update* 2000; 6: 225-36.
15. Brzozowski AM, Pike AC, Dauter Z, Hubbard RE, Bonn T, Engstrom O, et al. Molecular basis of agonism and antagonism in the oestrogen receptor. *Nature* 1997; 389: 753-8.
16. Pike AC, Brzozowski AM, Hubbard RE. A structural biologist's view of the oestrogen receptor. *J Steroid Biochem Mol Biol* 2000; 74: 261-8.
17. Ghafourian T, Cronin MT. Comparison of electrotopological-state indices versus atomic charge and superdelocalisability indices in a QSAR study of the receptor binding properties of halogenated estradiol derivatives. *Mol Divers* 2004; 8: 343-55.
18. Islam M, Pal R, Hossain T, Mukherjee A, Saha A. Molecular modeling studies on structural requirement of diarylpropionitrile for selectivity to estrogen receptor subtypes *Med Chem Res* 2011 (published online).
19. Mukherjee S, Nagar S, Mullick S, Mukherjee A, Saha A. Pharmacophore mapping of arylbenzothioephene derivatives for MCF cell inhibition using classical and 3D space modeling approaches. *J Mol Graph Model* 2008; 26: 884-92.
20. Mukherjee S, Nagar S, Mullick S, Mukherjee A, Saha A. Pharmacophore mapping of selective binding affinity of estrogen modulators through classical and space modeling approaches: exploration of bridged-cyclic compounds with diarylethylene linkage. *J Chem Inf Model* 2007; 47: 475-87.
21. Mukherjee S, Saha A, Roy K. QSAR of estrogen receptor modulators: exploring selectivity requirements for ER(alpha) versus ER(beta) binding of tetrahydroisoquinoline derivatives using E-state and physicochemical parameters. *Bioorg Med Chem Lett* 2005; 15: 957-61.
22. Wolohan P, Reichert DE. CoMSIA and docking study of rhenium based estrogen receptor ligand analogs. *Steroids* 2007; 72: 247-60.
23. Wolohan P, Reichert DE. CoMFA and docking study of novel estrogen receptor subtype selective ligands. *J Comput Aided Mol Des* 2003; 17: 313-28.
24. Sadler BR, Cho SJ, Ishaq KS, Chae K, Korach KS. Three-dimensional quantitative structure-activity relationship study of nonsteroidal estrogen receptor ligands using the comparative molecular field analysis/cross-validated r2-guided region selection approach. *J Med Chem* 1998; 41: 2261-7.
25. Fang H, Tong W, Shi LM, Blair R, Perkins R, Branham W, et al. Structure-activity relationships for a large diverse set of natural, synthetic, and environmental estrogens. *Chem Res Toxicol* 2001; 14: 280-94.
26. Wold S, Eriksson L. *Chemometric Methods*. Weinheim: VCH Verlagsgesellschaft mbh; 1995.
27. Friesner RA, Banks JL, Murphy RB, Halgren TA, Klicic JJ, Mainz DT, et al. Glide: a new approach for rapid, accurate docking and scoring. 1. Method and assessment of docking accuracy. *J Med Chem* 2004; 47: 1739-49.
28. Verma J, Khedkar VM, Coutinho EC. 3D-QSAR in drug design--a review. *Curr Top Med Chem* 2010; 10: 95-115.
29. Cramer R, Patterson D, Bunce J. Comparative molecular field analysis (CoMFA). 1. Effect of shape on binding of steroids to carrier proteins. *J Am Chem Soc* 1988; 110: 5959-5967.
30. Klebe G, Abraham U, Mietzner T. Molecular similarity indices in a comparative analysis (CoMSIA) of drug molecules to correlate and predict their biological activity. *J Med Chem* 1994; 37: 4130-46.
31. Martin Y. 3D QSAR: Current state, scope, and limitations. *Persp Drug Discov Des* 1998; 12: 3-23.
32. Debnath AK. Quantitative structure-activity relationship (QSAR) paradigm--Hansch era to new millennium. *Mini Rev Med Chem* 2001; 1: 187-95.
33. Bohm M, St rzebecher J, Klebe G. Three-dimensional quantitative structure-activity relationship analyses using comparative molecular field analysis and comparative molecular similarity indices analysis to elucidate selectivity differences of inhibitors binding to trypsin, thrombin, and factor Xa. *J Med Chem* 1999; 42: 458-77.
34. Yang GF, Huang X. Development of quantitative structure-activity relationships and its application in rational drug design. *Curr Pharm Des* 2006; 12: 4601-11.
35. Lushington GH, Guo JX, Wang JL. Whither combine? New opportunities for receptor-based QSAR. *Curr Med Chem* 2007; 14: 1863-77.
36. Dean PM, Lloyd DG, Todorov NP. De novo drug design: integration of structure-based and ligand-based methods. *Curr Opin Drug Discov Devel* 2004; 7: 347-53.
37. RCSB Protein Data Bank (<http://www.rcsb.org/pdb>).
38. Mocklinghoff S, van Otterlo WA, Rose R, Fuchs S, Zimmermann TJ, Dominguez Seoane M, et al. Design and evaluation of fragment-like estrogen receptor tetrahydroisoquinoline ligands from a scaffold-detection approach. *J Med Chem* 2011; 54: 2005-11.
39. Hoffmann R. An Extended Hückel Theory. I. Hydrocarbons. *J Chem Phys* 1963; 37: 1397-1412.
40. Brooijmans N, Kuntz ID. Molecular recognition and docking algorithms. *Annu Rev Biophys Biomol Struct* 2003; 32: 335-73.
41. Exner T, Brickmann J. New docking algorithm based on fuzzy set theory *J Mol Model* 1997; 3: 321-324.
42. Kinoshita K, Nakamura H. Identification of protein biochemical functions by similarity search using the molecular surface database eF-site. *Prot Sci* 2003;12(8):1589-95.
43. Wallace AC, Borkakoti N, Thornton JM. TESS: a geometric hashing algorithm for deriving 3D coordinate templates for searching structural databases. Application to enzyme active sites. *Prot Sci* 1997; 6: 2308-23.
44. Stockman G. Object recognition and localization via pose clustering. *Comp Vis Graph Image Process* 1987; 40: 361-387.
45. Friesner RA, Murphy RB, Repasky MP, Frye LL, Greenwood JR, Halgren TA, et al. Extra precision glide: docking and scoring incorporating a model of hydrophobic enclosure for protein-ligand complexes. *J Med Chem* 2006; 49: 6177-96.
46. Halgren TA, Murphy RB, Friesner RA, Beard HS, Frye LL, Pollard WT, et al. Glide: a new approach for rapid, accurate docking and scoring. 2. Enrichment factors in database screening. *J Med Chem* 2004; 47: 1750-9.
47. Zhou Z, Felts AK, Friesner RA, Levy RM. Comparative performance of several flexible docking programs and scoring functions: enrichment studies for a diverse set of pharmaceutically relevant targets. *J Chem Inf Model* 2007; 47: 1599-608.
48. Islam MA, Nagar S, Das S, Mukherjee A, Saha A. Molecular design based on receptor-independent pharmacophore: application to estrogen receptor ligands. *Biol Pharm Bull* 2008; 31: 1453-60.

